Article

New Method for Solving the Inverse Thermal Conduction Problem (θ-Scheme Combined with CG Method under Strong Wolfe Line Search)

Rachid Djeffal [1], Djemoui Lalmi [2,*], Sidi Mohammed El Amine Bekkouche [1], Tahar Bechouat [3] and Zohir Younsi [4,5]

[1] Unité de Recherche Appliquée en Energies Renouvelables, URAER, Centre de Développement des Energies Renouvelables, CDER, Ghardaïa 47133, Algeria

[2] Research Laboratory Materials, Energy Systems Technology and Environment (MESTEL), Université de Ghardaia, Rue de l'aeroport Noumerate, Ghardaia 47000, Algeria

[3] Department of Mathematics and Informatics, Faculty of Science and Technology, Mohammed Cherif Messaadia University, Souk Ahras 41000, Algeria

[4] FUPL, Hautes Etudes d'Ingénieur (HEI), LGCgE (EA 4515), Rue de Toul, F-59000 Lille, France

[5] Laboratoire Génie Civil & Geo-Environnement LGCgE-EA 4515, University of Artois, Technoparc Futura, F-62400 Béthune, France

* Correspondence: eldjemoui@gmail.com

Abstract: Most thermal researchers have solved thermal conduction problems (inverse or direct) using several different methods. These include the usual discretization methods, conventional and special estimation methods, in addition to simple synchronous gradient methods such as finite elements, including finite and special quantitative methods. Quantities found through the finite difference methods, i.e., explicit, implicit or Crank–Nicolson scheme method, have also been adopted. These methods offer many disadvantages, depending on the different cases; when the solutions converge, limited range stability conditions. Accordingly, in this paper, a new general outline of the thermal conduction phenomenon, called (θ-scheme), as well as a gradient conjugate method that includes strong Wolfe conditions has been used. This approach is the most useful, both because of its accuracy (16 decimal points of importance) and the speed of its solutions and convergence; by addressing unfavorable adverse problems and stability conditions, it can also have wide applications. In this paper, we applied two approaches for the control of the boundary conditions: constant and variable. The θ-scheme method has rarely been used in the thermal field, though it is unconditionally more stable for θ∈ [0.5, 1]. The simulation was carried out using Matlab software.

Keywords: thermal conduction; inverse problem; θ-scheme; CG method; Wolfe conditions; unconditionally stable

1. Introduction

In order to model a mathematical system that can solve a direct problem, it is necessary to look for factors that control the response of the system to several basic and necessary conditions. The latter are generally represented through: (1) The considered field engineering; (2) The equations that govern this area; (3) All temporal and spatial conditions that govern the area; (4) Properties of materials; and finally, (5) The sources that control and function in the field of study. At some times, one or more of the previous data that are necessary to solve the above direct problem are completely or partially absent. Thus, one can look for the missing data, and then should move to solving the reverse problem according to the theoretical data or find an analogous way to uncover the information related to the system's responses [1]. Generally, inverse problems are known problems that are more difficult to solve compared to direct problems; they may also suffer from the lack of an optimal selection, making them a complex problem. A lack of uniqueness and/or a lack of

solutions, or an instability of the solution to small problems that are due to changes in the provided data (disturbance) can lead to major problems with solutions [2].

To solve the problem of heat transfer through walls, Layal-Chahwane and al [3] presented an inverse method that estimated their thermal properties by adopting the limited difference method through the simspark environment program [4]. A good agreement was found between the direct and the reverse methods [5]. Jingbo Wang and al [6] studied the problems in evaluating parameters, rebuilding thermal history (including thermal flow at the borders), and rebuilding the heat source. This work was conducted using the joint probability distribution approach to determine the status of the conditional state (on the data) of unknown quantities by multiplying the previous probability and distribution functions. Bayesian hierarchical models were introduced to simplify earlier assumptions about the unknown quantities. The presented methods are general and applied for a number of inverse engineering problems.

A.S.A. Alghamdi [7] investigated the heat flow at the boundary; the inverse method of the heat conduction model was used by developing a direct and inverse mathematical model of a flat-panel probe that was subjected to time-dependent heat flow at one end while keeping the other side isolated. In this paper, the inverse algorithm that used the Levenberg–Marquardt method was applied. Thus, a satisfactory solution was found between the measured and estimated features of heat flow. The experiments were undertaken at the University of Ohio [8].

Solving "direct problems" allows the stimulation of physical phenomena in modeling, and if the phenomenon is governed by partial differential equations, different digital techniques can be used [9]. The most famous elements are finite, and finite differences are one of the most recent methods of boundary elements [10]. This considers that, depending on the endowment encountered in each process, many industrial studies require a solution to "inverse problems" and not a solution to "direct problems" [11]. This applies, for instance, to determining temperatures or contour flows according to internal measurements of the body, such as ovens and space missions [12].The main advantage of using inverse methods depends on various applications for problems that cannot be solved using other traditional methods. These include, for example, space shuttles, phase change materials, and thermal ovens.

Since it is widely known that many inverse problems in the physical sciences are ill-posed in the sense that the solution loses stability with respect to data perturbations and even minor perturbations of data can change the solution drastically. Generally, these types of perturbations come from measuring, rounding errors, and observation. Thus, the numerical solutions of these inverse problems are extremely susceptible to perturbations due to the poor posing of these problems [13]. For this reason, we're interested in considering the problem of heat transfer with noisy data. Therefore, the direct numerical approaches are not applicable to computing an appropriate solution for this type of problem. Regularization procedures should be used to solve an ill-posed problem with noisy data.

To extract valuable and relevant information from the model presented by heat transfer, the numerical solution to these problems necessitates the application of discretization strategies. This can be achieved in one of two ways: regularization-discretization (RD) or discretization-regularization (DR). In this paper, we will adopt the second strategy. In general, discretization methods treat linear or nonlinear ill-posed problems by transforming these problems into finite-dimensional systems. This discretization gives rise to ill-conditioned linear or nonlinear systems of algebraic equations. In most situations, the obtained systems must be regularized to compute the best approximation solution available [14].

The conjugate gradient method is known as one of the most powerful methods for the optimization of both linear and non-linear algebraic systems. For this reason, the conjugate gradient method is considered a regularized strategy for solving difficult linear or non-linear algebraic systems.

The explicit and implicit methods, as we all know, are strong tools for solving numerical approximations to the solutions of time-dependent ordinary and partial differential equations. These numerical methods are considered one of the most famous approximate methods for solving well-posed problems because of their ease of application.

In this work, the discretization method is a θ-scheme method, which is a combination of the previous methods. We then apply the conjugate gradient method as a strategy of regularization.

Our contribution adopted solutions for the problem of inverse thermal conductivity in a new, interesting, and accurate way (16 significant decimal digits) called (θ-scheme), paired with a gradient correlated with strong Wolfe conditions, using ($\theta \in [0.5, 1]$). On the other hand, most thermal researchers used simple graphs to estimate the value (explicit $\theta = 0$, implicit $\theta = 1$ and Crank–Nicolson $\theta = 0.5$), with a simple conjugate gradient, and these return several defects (stability and convergence state, limited application, etc.). Adding to the current contribution, both approaches were used to control boundary conditions: the inverse method, and fixed conditions where one capture was used. In the second approach, multiple pickups were used. Two pickups were selected: one on the hot side and the other on the cold side. Suggestions related to these terms are based on real data collected by our research team members, affiliated to *AERMASA_URAER*. Ghardaia carried out on an experimental platform that was implemented in the District buildings.

2. The Mathematical Procedure

In this paper, the work proposed addresses the heat transfer in a wall built from stone, which is purely conductive and unidirectional as well as adiabatic at the top and the bottom side (isolate), as shown in Figure 1a. With the objective of controlling the boundary conditions of the wall, the study adopted two approaches: the first approach uses the constant conditions and the second one uses the real conditions [15]. These conditions are not chosen arbitrarily but are based on the real data drawn from several experiments on a dwelling house of a functional nature within the Applied Research Unit for Renewable Energies (*URAER*), Ghardaïa, Figure 1b [16]. Figure 2a,b show the inside and outside temperature evolution in the study house for 29 June 2007 and 15 July 2007.It can be seen the temperature can be exceed 40 °C and also the the comparison between the outside temperature the calculation is satisfactory.

(**a**)   (**b**)

Figure 1. (**a**) Thermocouple position in room [15,16], (**b**) radiometric station in Uraer [17].
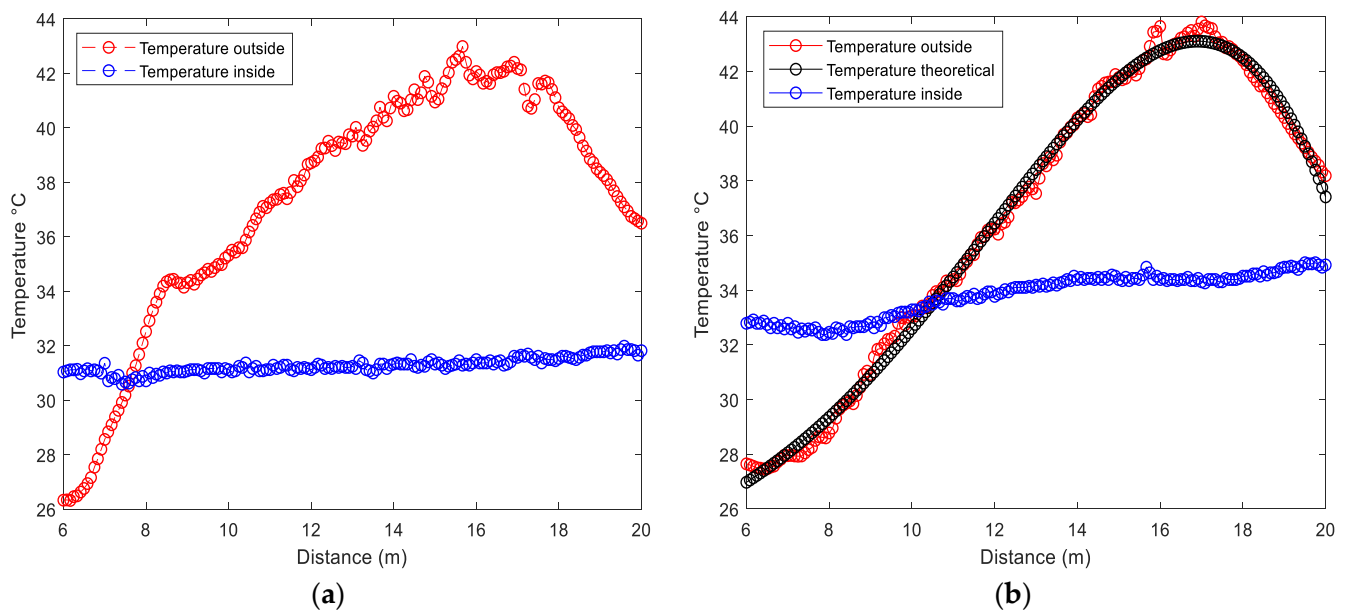
Figure 2. Real temperature evolution (experimental) (**a**) 29 June 2007; (**b**) 15 July 2007.

2.1. Validation of the Procedure

In this validation, the evolution of temperatures was compared in a wall made of hard stone, determined by both direct and inverse methods, after the third iteration. The obtained results are almost identical, Figure 3.
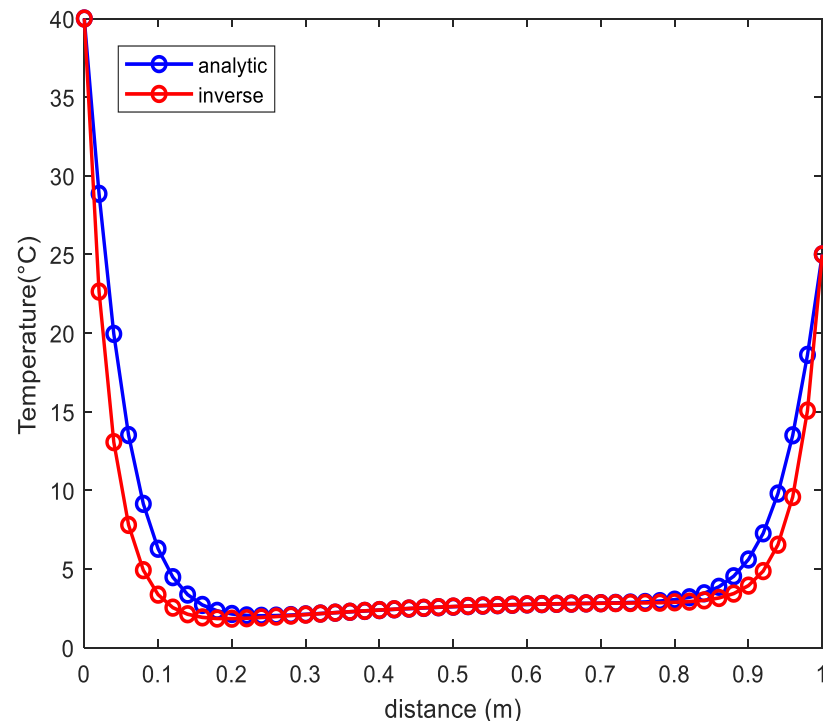

Figure 3. Validation of the inverse and analytical method.

2.2. Direct Procedure

To solve a direct problem in a mathematical system, it is necessary to look for the factors that control the system's response to several basic and necessary conditions. The latter are generally represented by: (1) the geometry of the land considered. (2) The

equations that govern this domain. (3) All the governing spatial-temporal conditions. (4) Properties of materials and finally the sources that control and work in the field of study.

The problem treated in this study deals essentially with an unsteady thermal conduction, which is governed by the following unidirectional partial differential equation:

$$k\frac{\partial^2 T}{\partial x^2} + f_0 = \rho C_p \frac{\partial T}{\partial t} \tag{1}$$

where $0 \leq x \leq e$ and f_0 a heat sources.

In association with the previous equation, the examined wall is subject to the following boundary and initial conditions:

$$\begin{cases} T(x,t) = T_0 \ \ or -k\frac{\partial T}{\partial x} = q(x,t) \ at \ x = 0 \\ \qquad T(x,t) = T_e \ \ at \ x = e \\ \qquad T(x,t) = F(x) \ \ for \ t = 0 \end{cases}$$

Figure 4 shows the physical representation of the problem under consideration. The stone wall was 0.4 m thick. Initially, the ambient temperature was 20 °C. The supposed boundaries conditions are located at $x = 0$ m, where the hot temperature $Tc = T_0 = 40$ °C, and at $x = 0.4$ m, the wall was maintained at room temperature $T_f = T_e = 25$ °C.
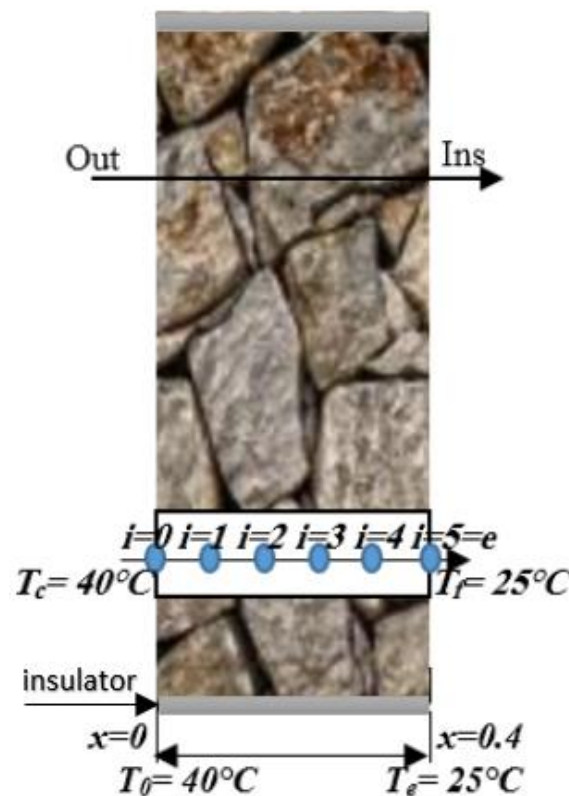

Figure 4. Boundary conditions and direct problem position.

The thermos-physical properties of the stone used are [18]: $\rho = 2000 \ kgm^{-3}$, $C_p = 1000 \ jkg^{-1}k^{-1}$ and $k = 2.3 \ wm^{-1}k^{-1}$.

To determine the temperature evolution in the wall with the direct method, three different schemes were adopted: explicit, implicit and the theta scheme.

2.3. Explicit Form

One can discretize Equation (1) to determine the evolution of temperature $T(t, x)$ in the explicit form of the finite differences according to Figure 5, using the following approximation: $\frac{\partial T}{\partial t} \approx \frac{T_i^{n+1} - T_i^n}{\Delta t}$ and $\frac{\partial^2 T}{\partial x^2} \approx \frac{T_{i+1}^n - 2T_i^n + T_{i-1}^n}{\Delta x^2}$.
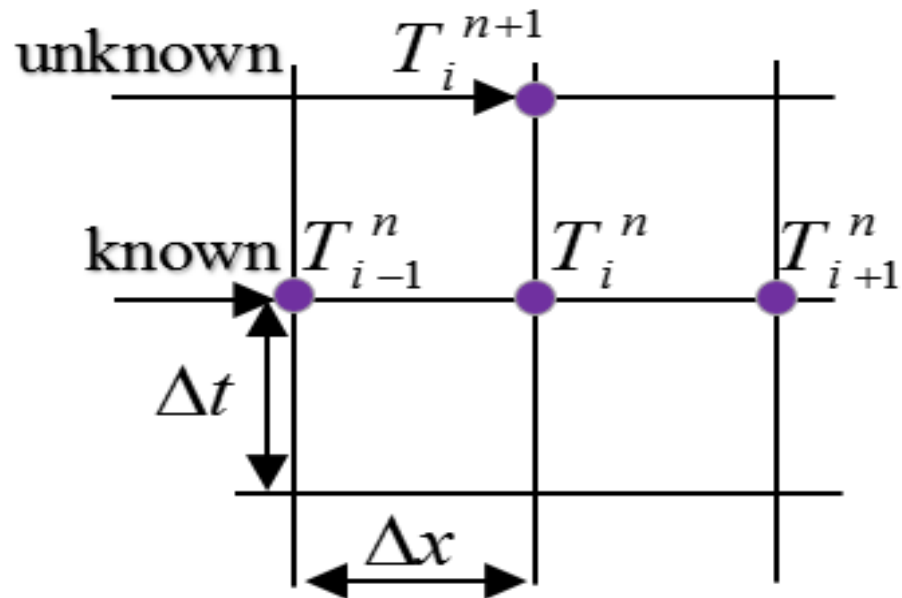

Figure 5. Explicit scheme of finite differences Discretization.

The discretization equation can be written in the following form:

$$T_i^{n+1} = DT_{i+1}^n + (1 - 2D)T_i^n + DT_{i-1}^n \tag{2}$$

where $n = 0, 1, 2, \ldots, M$ and $i = 1, 2, \ldots, N$, $D = \alpha \frac{\Delta t}{\Delta x^2}$ and $\alpha = \frac{k}{\rho C_p}$.

Equation (2) is the explicit form obtained using the finite differences method discretization. This form is stable when $(1 - 2D) \leq 0$. After the introduction of the boundary conditions, this equation can be written in matrix form as follows:

$$T^{n+1} = AT^n + B \tag{3}$$

where $A = \begin{bmatrix} \gamma & D & 0 & \cdots & \cdots & 0 \\ D & \gamma & D & \ddots & \ddots & \vdots \\ 0 & D & \gamma & D & \ddots & \vdots \\ \vdots & \ddots & \ddots & \ddots & \ddots & 0 \\ \vdots & \ddots & \ddots & D & \gamma & D \\ 0 & \cdots & \cdots & 0 & D & \gamma \end{bmatrix}$, $B = \begin{bmatrix} DT_0 \\ 0 \\ \vdots \\ \vdots \\ 0 \\ DT_e \end{bmatrix}$ and $\gamma = 1 - 2D$.

The calculation starts with $n = 0$. So, we calculate T_i^1 for $i = 1, \ldots, N$ through Equation (2). In this step, the instantaneous temperature is calculated based on the initial temperature and the boundary conditions.

For the second step, we use $n = 1$ and calculate T_i^2 for $i = 1, \ldots, N$ using the temperatures calculated in the previous step.

This operation is repeated for each time step, until reaching a thermally steady state defined by an invariant temperature profile (Figure 6). Figure 7 shows the obtained absolute error using the finite difference method.
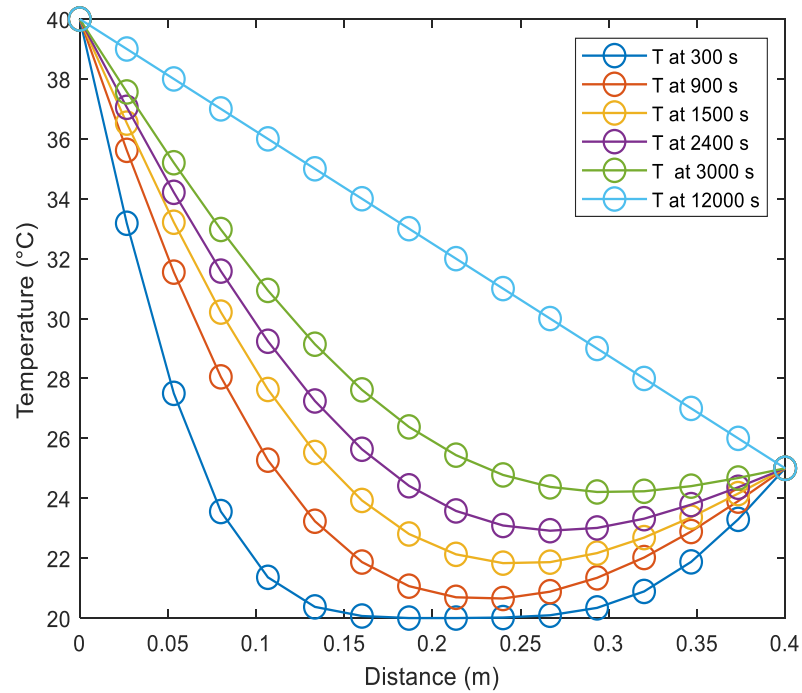
Figure 6. Temperature evolution using the explicit form of finite difference method.
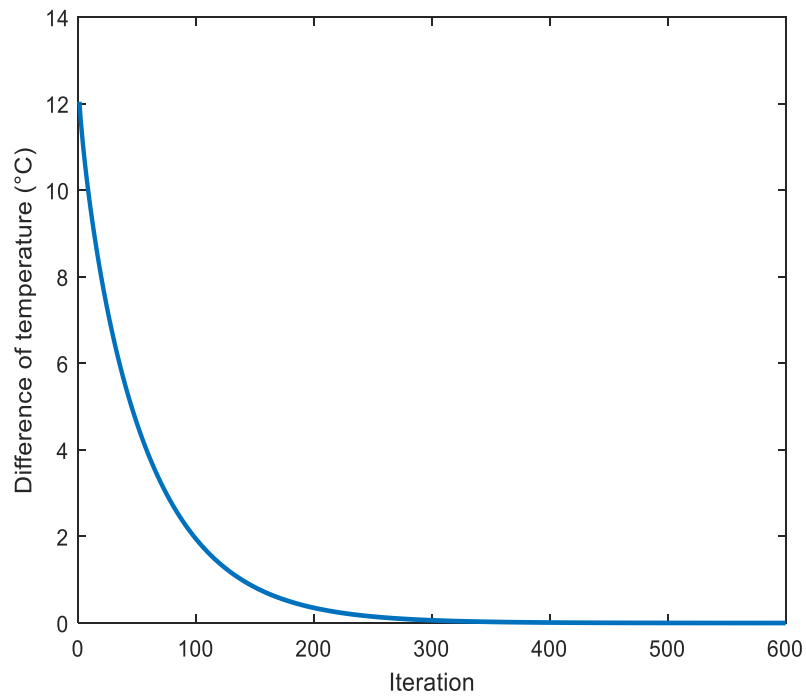

Figure 7. Absolute Error using the explicit form of finite differences method.

2.4. Implicit Form

To resolve the direct problem, the implicit centered finite difference method was used to discretize the latter Equation (1), (Figure 8).

Using backward difference in time and second-order central difference of the space derivative, we obtain the implicit scheme as shown below:

$$\frac{T_i^{n+1} - T_i^n}{\Delta t} = \alpha \frac{T_{i+1}^{n+1} - 2T_i^{n+1} + T_{i-1}^{n+1}}{\Delta x^2}$$

After reorganization, we find

$$- DT_{i+1}^{n+1} + (1 + 2D)T_i^{n+1} - DT_{i-1}^{n+1} = 0 \qquad (4)$$

where: $n = 0, 1, 2, \ldots, M$ and $i = 1, 2, \ldots, N$; $D = \alpha \frac{\Delta t}{\Delta x^2}$ and $\alpha = \frac{k}{\rho C_p}$
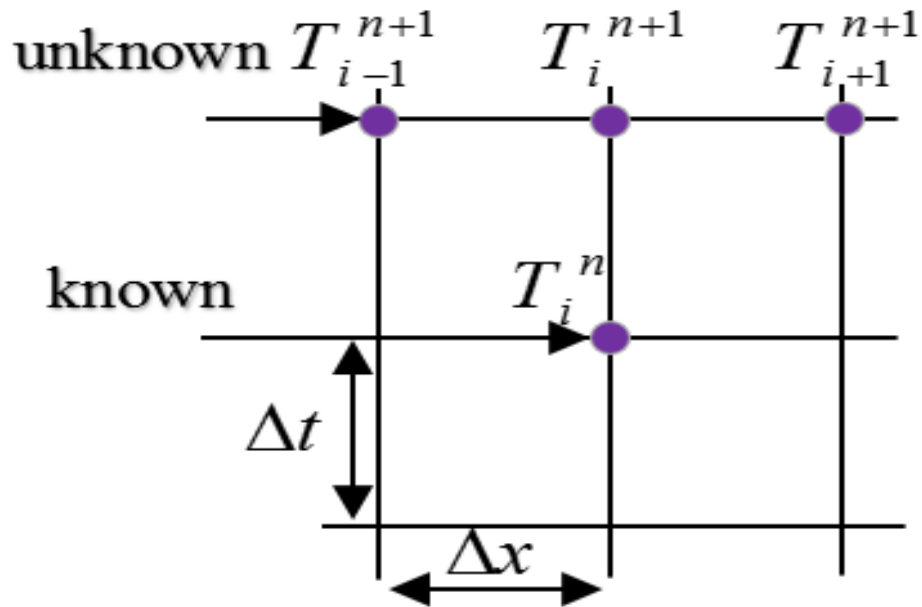

Figure 8. Implicit scheme of finite difference discretization.

The implicit scheme is unconditionally stable, so we can choose dt and dx independently. After introduction of the boundary conditions, Equation (4) can be written in the following matrix form:

$$AT^{n+1} = B \qquad (5)$$

with

$$A = \begin{bmatrix} \gamma & -D & 0 & \cdots & \cdots & 0 \\ -D & \gamma & -D & \ddots & \ddots & \vdots \\ 0 & -D & \gamma & -D & \ddots & \vdots \\ \vdots & \ddots & \ddots & \ddots & \ddots & 0 \\ \vdots & \ddots & \ddots & -D & \gamma & -D \\ 0 & \cdots & \cdots & 0 & -D & \gamma \end{bmatrix}, \quad B = \begin{bmatrix} T_1^n + DT_0 \\ T_2^n \\ \vdots \\ \vdots \\ T_{N-1}^n \\ T_N^n + DT_e \end{bmatrix}$$

and

$$\gamma = 1 + 2D$$

To determine the temperature evolution in the wall using the implicit method, it is necessary to solve the algebraic system obtained by Equation (5). In this study, we have adopted the Thomas algorithm (tri-diagonal matrix algorithm) [18–20]. The obtained results are plotted in Figure 9 at different times. The absolute error was plotted in Figure 10. It can be seen that the implicit form of the finite difference method exhibited faster convergence than the explicit form.
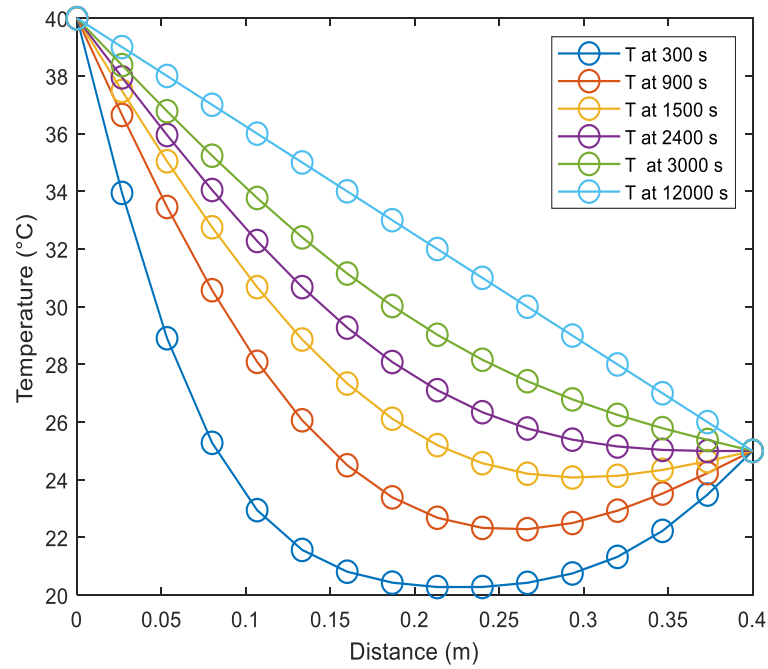
Figure 9. Temperature evolution using the implicit finite difference method.
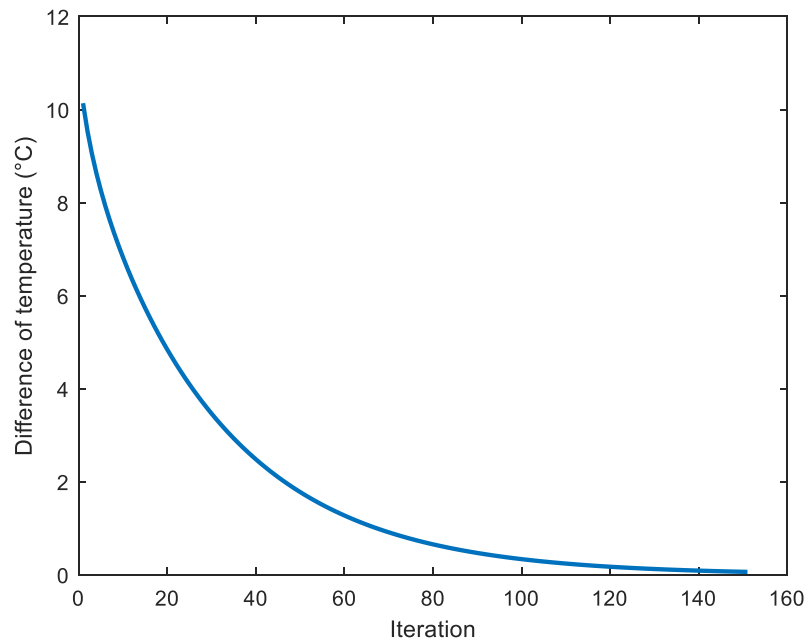
Figure 10. Absolute Error using the implicit form of finite differences method.

2.5. Crank–Nicolson Form

The Crank–Nicolson method is a special case of the so-called θ-scheme $(\theta = 0.5)$, which can be briefly defined as an implicit and unconditionally stable approximation (Figure 11). It considers the second order in time and space [21,22].

$$\frac{1}{\alpha}\frac{T_i^{n+1} - T_i^n}{\Delta t} = \frac{1}{\Delta x^2}\left[\theta\left(T_{i-1}^n - 2T_i^n + T_{i+1}^n\right) + (1-\theta)\left(T_{i-1}^{n+1} - 2T_i^{n+1} + T_{i+1}^{n+1}\right)\right]$$

Figure 11. Distribution of Nodes using the Crank–Nicolson scheme.

After rearrangement and setting $\theta = 0.5$, we find:
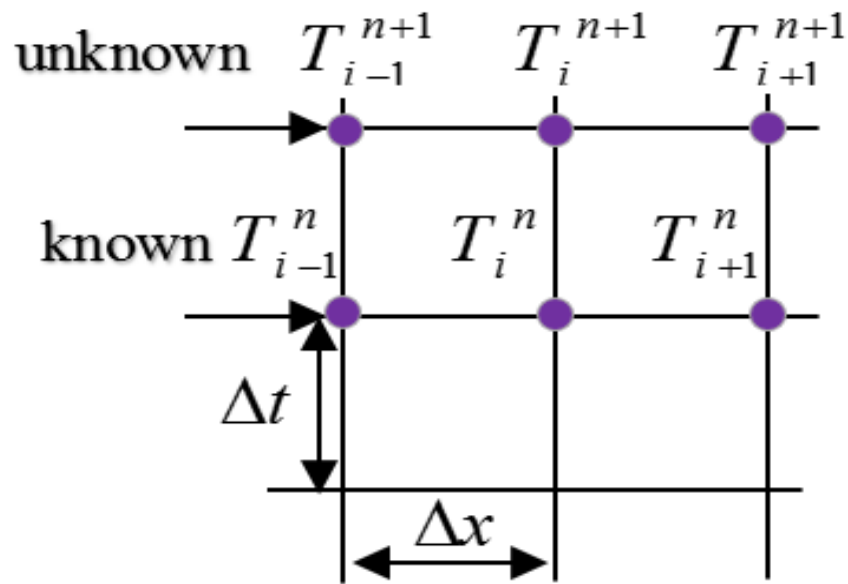
$$- DT_{i+1}^{n+1} + (1 + 2D)T_i^{n+1} - DT_{i-1}^{n+1} = DT_{i+1}^n + (1 - 2D)T_i^n + DT_{i-1}^n \tag{6}$$

where n, i, α and D are $n = 0, 1, 2, \ldots, M, i = 1, 2, \ldots, N, D = 2\frac{\alpha\Delta t}{\Delta x^2}, \alpha = \frac{k}{\rho C_p}$.

After boundary conditions are introduced, Equation (6) can be written in the following algebraic equations system, and Equation (7) in matrix form:

$$AT^{n+1} = BT^n + C \tag{7}$$

where

$$A = \begin{bmatrix} \gamma_A & -D & 0 & \cdots & \cdots & 0 \\ -D & \gamma_A & -D & \ddots & \ddots & \vdots \\ 0 & -D & \gamma_A & -D & \ddots & \vdots \\ \vdots & \ddots & \ddots & \ddots & \ddots & 0 \\ \vdots & \ddots & \ddots & -D & \gamma_A & -D \\ 0 & \cdots & \cdots & 0 & -D & \gamma_A \end{bmatrix}, \; B = \begin{bmatrix} \gamma_B & D & 0 & \cdots & \cdots & 0 \\ D & \gamma_B & D & \ddots & \ddots & \vdots \\ 0 & D & \gamma_B & D & \ddots & \vdots \\ \vdots & \ddots & \ddots & \ddots & \ddots & 0 \\ \vdots & \ddots & \ddots & D & \gamma_B & D \\ 0 & \cdots & \cdots & 0 & D & \gamma_B \end{bmatrix}, \; C = \begin{bmatrix} 2DT_0 \\ 0 \\ \vdots \\ \vdots \\ 0 \\ 2DT_e \end{bmatrix},$$

$\gamma_A = 1 + 2D$ and $\gamma_B = 1 - 2D$.

Figures 12 and 13 show the temperature evolution and absolute error using the Crank–Nicolson form of the finite difference method. It can be seen that the three methods seem stable, but the stability of the explicit method is present at a well-defined interval [0, 0.5]. On the other hand, the two other methods (implicit and Crank–Nicolson) are unconditionally stable. On the convergence side, the Crank–Nicolson method is the fastest convergence method (after 145 iterations) and the implicit method (after 150 iterations), but the explicit method converges only after 300 iterations (Table 1).

Table 1. Summary of some results for the three methods.

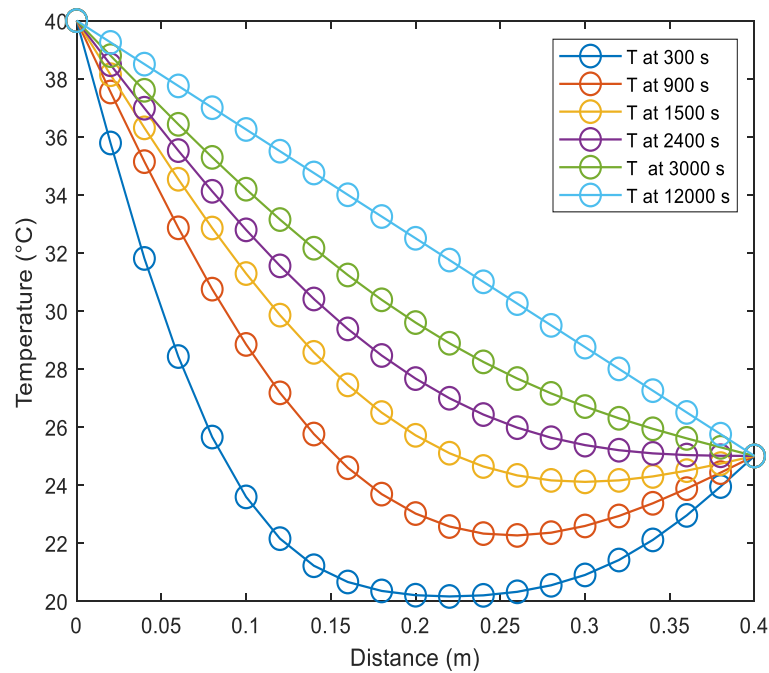| Methods	Explicit Form	Implicit Form	Crank–Nicolson Form
Elapsed time (s)	0.671737	0.501063	0.567344
iteration of convergence	300	150	145

Figure 12. Temperatures evolution using Crank–Nicolson form of the finite difference method.
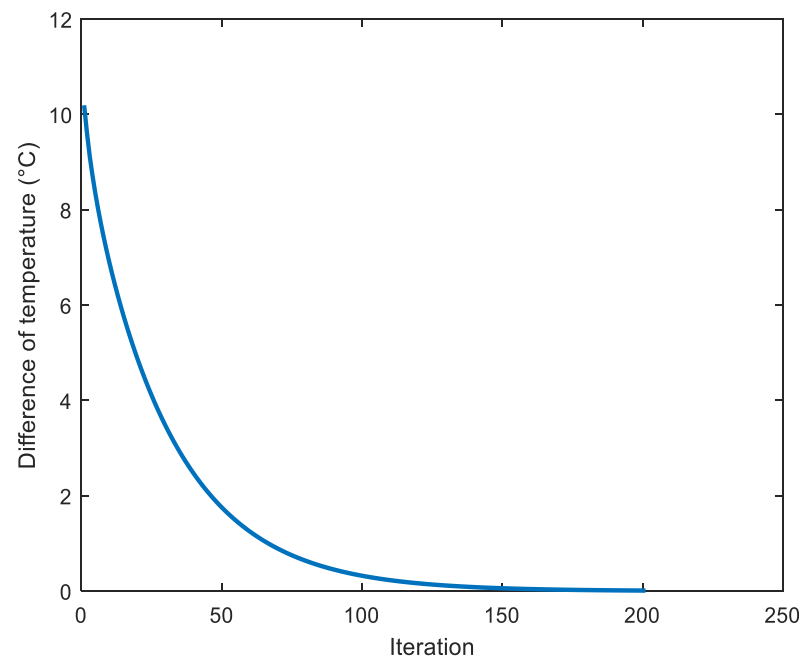

Figure 13. Absolute Error using Crank–Nicolson form of the finite differences.

2.6. Inverse Procedure of θ-Scheme

Inverse problems in general are known problems that have been poorly posed and are more difficult to solve compared to direct problems. In case one or more of the previous data required to solve the direct problem mentioned above are totally or partially missing, and we are looking for the missing data return, then we need to tackle the reverse problem to solve it according to the method used to find the information (theoretical or analogous) linked to the responses of this system. The lack of an optimal selection for a bad problem, either as a lack of uniqueness and/or solutions, or when the instability of the solution to small problems of change in the presented data (disturbance) lead to major issues with the solutions.

- **Approach 1.**

The unknown boundary conditions are constant, Figure 14;

$$k\frac{\partial^2 T}{\partial x^2} = \rho C_p \frac{\partial T}{\partial t}, \ for \ 0 < x < e, \ t > 0 \tag{8}$$

with

$$\begin{cases} T(0,t) = T_0 = ?, \ x = 0, \ t > 0, \ unknown \ boundary \\ T(e,t) = T_e = ?, \ x = e, \ t > 0, \ unknown \ boundary \\ T(x,0) = F(x), \ 0 < x < e, \ t = 0, \ intial \ condition \end{cases}$$
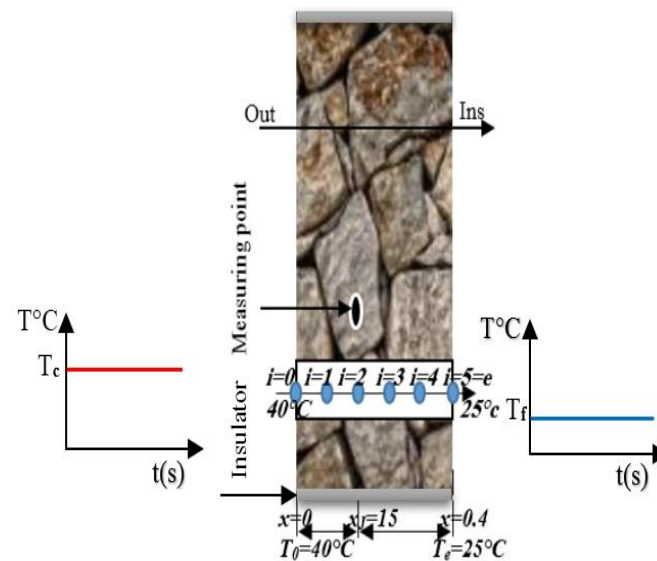

Figure 14. Physical representation of the inverse problem studied (Approach 1).

The use of the θ-scheme leads to the following relations:

$$\begin{cases} (1+2D\theta)T_1^{n+1} - D\theta T_2^{n+1} = -(1-2D(1-\theta))T_1^n + D(1-\theta)T_2^n + DT_0 \\ -D\theta T_{i-1}^{n+1}(1+2D\theta)T_1^{n+1} - D\theta T_{i+1}^{n+1} = D(1-\theta)T_{i-1}^n - \\ (1-2D(1-\theta))T_1^n + D(1-\theta)T_{i+1}^n \quad for \ i = 2,\dots,N-1 \\ -D\theta T_{N-1}^{n+1} + (1+2D\theta)T_N^{n+1} = D(1-\theta)T_{N-1}^n - (1-2D(1-\theta))T_N^n + DT_e \end{cases} \tag{9}$$

where $D = \frac{k\Delta t}{\rho C \Delta x^2}$.

We note that:

- For θ = 0, the θ-scheme (8) gives the explicit scheme.
- For θ = 1, the θ-scheme (8) leads to the implicit scheme.
- If θ = 0.5, the θ-scheme (14) gives the Crank–Nicolson scheme.

The θ-scheme (8) is unconditionally stable for θ ∈ [0.5, 1], and it can be written in matrix form as follows:

$$A_\theta T^{n+1} = B_\theta T^n + Y \tag{10}$$

The relation thus gives the solution sought:

$$T^{n+1} = C_\theta T^n + A_\theta^{-1} Y \tag{11}$$

where $C_\theta = A_\theta^{-1} B_\theta$.

The solution of the conduction problem (10) with unknown boundary conditions T_0 and T_e is an inverse heat conduction problem. The objective of this method is to find the boundary conditions T_0 and T_e which allow the reproduction of the temperature

evolution $T_j^{mes} = \left(T_j^{1,m}, T_j^{2,m}, \ldots, T_j^{M,m}\right)^T$ to be determined experimentally at the location of coordinates x_j.

The solution of this inverse heat conduction problem for estimating the vector $Q = (T_0, T_e)^T$ is based on the minimization of the least-squares norm:

$$J(Q) = \|T_j^{mes} - T_j\|^2 = \sum_{i=1}^{M} \left(T_j^{i,m} - T_j^i\right)^2 \tag{12}$$

where $T_j = (\sum_{k=1}^{N} C_{j,k} T_k^{n-1} + A_{j,1}^{-1} DT_0 + A_{j,N}^{-1} DT_e)^T$ $n = 1, \ldots, M$; $T_j^{mes} = (T_j^{1,m}, T_j^{2,m}, \ldots, T_j^{M,m})^T$.

So, to recover the vector Q, we solve the following optimization problem:

$$\min_{Q \in \mathbb{R}^2} J(Q) \quad where \quad J(Q) : \mathbb{R}^2 \to \mathbb{R} \tag{13}$$

Many mathematical methods are adopted to solve minimization problems (12). The conjugate gradient (CG) method is one of the optimization methods often used in applied works such as the optimization problem (12). It is noted that J is a smooth nonlinear function, and its gradient is denoted by $g(Q) = \nabla J(Q)$.

To solve (12), the conjugate gradient method uses the following iterative formula:

$$Q^{k+1} = Q^k + \alpha_k \times d_k \quad k = 1, 2, \ldots \tag{14}$$

where Q^k is the current iteration point and $\alpha_k > 0$ is the step size obtained by some line search method, and d_k is the search direction defined by:

$$d_k = \begin{cases} -g_k & k = 1 \\ -g_k + \beta_k \times d_{k-1} & k \geq 2 \end{cases} \tag{15}$$

where β_k is a scalar and $g_k = g(Q_k)$.

One of the most common and popular approaches of the inaccurate online research technique is the so-called Wolfe line search.

The strong Wolfe line search introduced two conditions as follows:

$$\begin{cases} J\left(Q^{k+1}\right) \leq J\left(Q^k\right) + c_1 \alpha_k g_k^T d_k \\ \left|g_{k+1}^T d_k\right| \geq -c_2 g_k^T d_k \end{cases} \quad 0 < c_1, c_2 < 1 \tag{16}$$

Different formulas for the coefficient β_k determine different conjugate gradient (CG) methods. In [3,4], the coefficient $\beta_k = \beta_k^{PRP}$ is given by:

$$\beta_k^{PRP} = \frac{g_k^T (g_k - g_{k-1})}{\|g_{k-1}\|^2} \tag{17}$$

Generally, the problem of finding the best approximate solution to the inverse problem (7) is ill-posed because even minor perturbations of data can change the solution drastically and therefore the problem of finding the best solution is an unstable solution. The question is how to find a stable solution? The answer is simple: it depends on its regularization. To regularize an ill-posed problem, one needs to replace it with another approximate problem that is well posed so that the error made is offset by the gain in stability.

For the inverse ill-posed problems and to compensate for the information on the boundary conditions T_0 *and* T_e, we assume that the temperatures $T_j^{mes,\delta} = (T_j^{1,m} + \delta_1, T_j^{2,m} + \delta_2, \ldots, T_j^{M,m} + \delta_m)^T$ are given at an interior point x_j with the ad-

dition of measurement noise $\delta = (\delta_1, \delta_2, \ldots, \delta_m)^T$. In this case, the following optimization problem is solved as follows:

$$\min_{Q \in \mathbb{R}^2} \hat{J}(Q) \quad where \quad \hat{J}(Q) : \mathbb{R}^2 \to \mathbb{R} \tag{18}$$

with

$$\begin{cases} \hat{J}(Q) = \|T_j^{mes,\delta} - T_j\|_2^2 = \sum_{i=1}^{M} \left(\left(T_j^{i,m} + \delta_i \right) - T_j^i \right)^2 \\ T_j^{mes,\delta} = T_j^{mes} + \delta \times randn \left(size \left(T_j^{mes} \right) \right) \end{cases}$$

Observation: in our case the matrix is reversible and well placed.

The results grouped in Table 2 present and prove the reliability of this regular inverse method for the given problems, especially alongside unknown thermal problems (undetermined conditions).

Table 2. Summary of some results of regular inverse problems.

Epsilon	Initial Temperature		Inverse	Regulated Inverse	Inverse Error	Regulated Inverse Error
E = 0.0000001	T0 input	4 °C	40.0000	40.0000	0.0000000638	0.0000000166
	Te input		25.0000	25.0000	−0.0000003608	−0.0000001838
E = 0.0001	T0 input	10 °C	40.0000	40.0000	−0.0000000216	−0.0000157
	Te input		25.0000	25.0002	0.0000001495	0.0002190
E = 0.001	T0 input	5 °C	40.0000	39.9999	−0.0000000216	−0.0000924
	Te input		25.0000	24.9993	0.0000001495	−0.0007431

Table 3 presents the results of a test for comparison with the reverse method (method applied to a wall with two sides, one hot and the other cold). These obtained results indicate the speed of the method used in the resolution; wich parformed with great precision.

Table 3. Comparison between the results of inverse problems on the hot and cold sides at different iterations.

Number of Iterations	Temperature Hot Inverses	Temperature Cold Inverses	Absolute Error
2	39.9999563	24.9998974	1×10^{-5} (0.0423,0.7978)
50	39.9999987	24.9999998	1×10^{-5} (0.0956,−0.6285)
100	40.0000001	25.0000003	1×10^{-5} (−0.0381,0.2515)
150	40.0000000	25.0000000	1×10^{-6} (0.1404,−0.9407)
200	40.0000000	25.0000000	1×10^{-6} (0.1423,−0.9518)
250	40.0000000	25.0000000	1×10^{-5} (0.0533,−0.3558)
300	40.0000000	25.0000000	1×10^{-7} (−0.1730,0.1357)

In Figure 15a–e, it can be observed that the estimated graphs of the θ-scheme method converge and tend to move to the exact solution quickly, which clearly proves the power of this new θ-scheme method at different values of θ and different time steps. Note that the graphs of the exact solutions are identical to the inverse solutions. Therefore, the usefulness of this method easily converges to precise and stable solutions following the second or the third iteration in the interval [0.5, 1]. Meanwhile, in Figure 15f, we note that the scheme is unstable since we enter the interval of the explicit scheme (] 0, 0.5 [); the latter is conditionally stable.
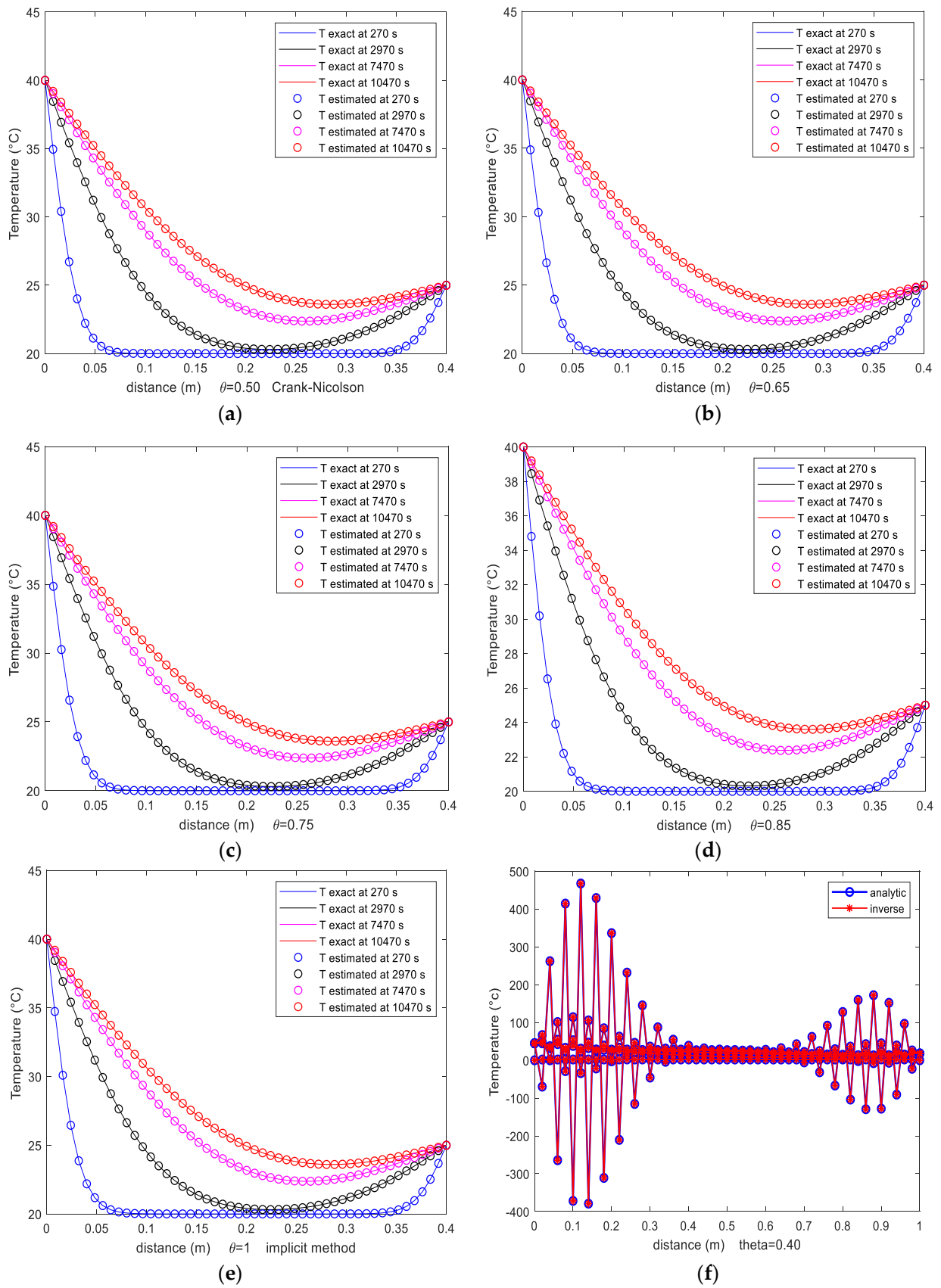
Figure 15. Temperatures evolution in different cases of θ-scheme; (**a**) *θ* = 0.50; (**b**) *θ* = 0.65; (**c**) *θ* = 0.75; (**d**) *θ* = 0.85; (**e**) *θ* = 1; (**f**) *θ* = 0.40.

- **Approach 2.**

  Figure 16 shows the unknown boundary conditions are variables:

$$k\frac{\partial^2 T}{\partial x^2} = \rho C_p \frac{\partial T}{\partial t}, \ for \ 0 < x < e, \ t > 0 \tag{19}$$

with

$$\begin{cases} T(0,t) = q_c(t), \ x = 0, \ t > 0, \ unknown \ boundary \\ T(e,t) = q_f(t), \ x = e, \ t > 0, \ unknown \ boundary \\ T(x,0) = F(x), \ 0 < x < e, \ t = 0, \ intial \ condition \end{cases}$$
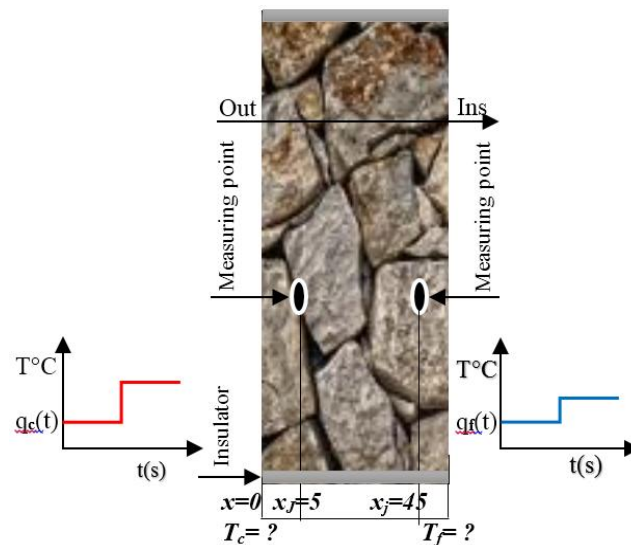

Figure 16. Boundary conditions of the inverse problems (Approach 2).

Using the implicit scheme, Equation (18) leads to the following algebraic system:

$$\begin{cases} (1+2D)T_1^{n+1} - DT_2^{n+1} = T_1^n + Dq_c^{n+1} \\ -DT_{i-1}^{n+1} + (1+2D)T_i^{n+1} - DT_{i+1}^{n+1} = T_i^n \ for \ i = 2,\ldots,N-1 \\ -DT_{N-1}^{n+1} + (1+2D)T_N^{n+1} = T_N^n + Dq_f^{n+1} \end{cases} \tag{20}$$

where $D = \frac{k\Delta t}{\rho C_p \Delta x^2} n = 1,\ldots, M-1$.

The matrix form of the system (19) is given by the relation:

$$AT^{n+1} = T^n + DY^{n+1} \tag{21}$$

The matrix form (20) can be written as:

$$T^{n+1} = BT^n + DBY^{n+1}$$

with

$$B = A^{-1}$$

The solution of the heat conduction problem (18) with the unknown boundary conditions q_c and q_f is an inverse heat conduction problem. To compensate for the information on the boundary conditions q_c and q_f, we assume that the temperatures $T_j^{mes} = (T_j^{1,m}, T_j^{2,m}, \ldots, T_j^{M,m})^T$ are given at l interior points x_j, $j = 1,\ldots,l$.

The solution of this inverse heat conduction problem for the estimation of the vectors $Q_c = (q_c^1, q_c^2, \ldots, q_c^M)^T$ and $Q_f = (q_f^1, q_f^2, \ldots, q_f^M)^T$ is based on the minimization of the least-squares norm:

$$J\left(Q_c, Q_f\right) = \sum_{j=1}^{l} \| T_j^{mes} - T_j \|^2 = \sum_{j=1}^{l} \sum_{i=1}^{M} \left(T_j^{i,m} - T_j^i\right)^2 \tag{22}$$

where
$$T_j^{n+1} = \sum_{k=1}^{N} B_{j,k} T_k^n + (D \times B)_{j,1} q_c^{n+1} + (D \times B)_{j,N} q_{cf}^{n+1}$$
$$T_j^{mes} = (T_j^1, T_j^2, \ldots, T_j^M)^T \qquad j = 1, \ldots, l.$$

So, to recover the vector $Q = \left(Q_c, Q_f\right)^T = (q_c^1, q_c^2, \ldots, q_c^M, q_f^1, q_f^2, \ldots, q_f^M)^T$, we solve the following optimization problem:

$$\min_{Q \in \mathbb{R}^{2M}} J(Q) \quad where\ J(Q) : \mathbb{R}^{2M} \to \mathbb{R} \tag{23}$$

To solve the optimization problem (22), we use the conjugate gradient method defined by (13), (14), (15), and (16) in Approach 1.

To calculate the gradient of $J(Q)$ given in (21), we use $k = 1, 2, \ldots, 2M$ to find the relation:

$$\frac{\partial}{\partial q_k} J(Q) = \frac{\partial}{\partial q_k} \sum_{j=1}^{l} \sum_{i=1}^{M} \left(T_j^{i,m} - T_j^i(Q)\right)^2 = \sum_{j=1}^{l} \sum_{i=1}^{M} -2 \frac{\partial}{\partial q_k} T_j^i(Q) \left(T_j^{i,m} - T_j^i(Q)\right) \tag{24}$$

where $Q = (q_c^1, q_c^2, \ldots, q_c^M, q_f^1, q_f^2, \ldots, q_f^M)^T = (q_1, q_2, \ldots, q_M, q_{M+1}, q_{M+2}, \ldots q_{2M})^T$. By simple calculation, we have the first derivative $\frac{\partial}{\partial q_k} T_j^i(Q)$ of $T_j^i(q_1, q_2, \ldots, q_{2M})$ for all $k = 1, \ldots, 2M$,

$$\frac{\partial}{\partial q_k} J(Q) = \begin{cases} \sum_{j=1}^{l} \sum_{i=1}^{M} -2C_j(k,i)(T_j^{i,m} - T_j^i(Q)) & \text{if } k = 1, 2, \ldots, M \\ \sum_{j=1}^{l} \sum_{i=1}^{M} -2E_j(k,i)(T_j^{i,m} - T_j^i(Q)) & \text{if } k = M+1, \ldots, 2M \end{cases}$$

where $C_j = D \times \begin{pmatrix} B_{j1} & 0 & \cdots & 0 \\ (B^2)_{j1} & B_{j1} & \cdots & 0 \\ \vdots & \ddots & \ddots & \vdots \\ (B^M)_{j1} & \cdots & (B^2)_{j1} & B_{j1} \end{pmatrix}$ and $E_j = D \times \begin{pmatrix} B_{jN} & 0 & \cdots & 0 \\ (B^2)_{jN} & B_{jN} & \cdots & 0 \\ \vdots & \ddots & \ddots & \vdots \\ (B^M)_{jN} & \cdots & (B^2)_{jN} & B_{jN} \end{pmatrix}$

Therefore, the gradient of the function $J(Q)$ is given by

$$\nabla J(Q) = (\frac{\partial}{\partial q_1} J(Q), \frac{\partial}{\partial q_2} J(Q), \ldots, \frac{\partial}{\partial q_M} J(Q), \ldots, \frac{\partial}{\partial q_{2M}} J(Q))^T$$

Numerical Results

All computations were carried out in Matlab with about 16 significant decimal digits. In these examples, we chose:

$$\varepsilon = 10^{-2}; Q^1 = m \times (1, 1, \ldots, 1)^T\ m = 1, 2, \ldots; c_1 = 10^{-3}, c_2 = 10^{-4}\ and\ l = 2.$$

Example:

In this example, let

$$\rho = 2000; c = 1000; \lambda = 2.3; L = 0.4\ and\ t_{final} = 12,000$$
$$T(x, 0) = F(x) = 20; r_1 = 5, r_2 = 45, N = 50; M = 40.$$

And let

$$q_c(t) = \begin{cases} 25/12{,}000 \times t + 35 & if\ 0 < t \leq 4800 \\ -12.5/12{,}000 \times t + 50 & if\ 4800 < t \leq 9600 \\ 40 & if\ 9600 < t \leq 12{,}000 \end{cases}$$

$$q_f(t) = \begin{cases} 15/12{,}000 \times t + 35 & if\ 0 < t \leq 2400 \\ 25 & if\ 2400 < t \leq 9600 \\ -15/12{,}000 \times t + 35 & if\ 9600 < t \leq 12{,}000 \end{cases}$$

Figures 17 and 18 show that the perturbations exist only in the beginning and at the end of the graphs. Despite the boundary conditions, they are variable. All this demonstrates the reliability and the power of convergence of this method. We can also see that the graphs are similar for exact solutions and estimation.
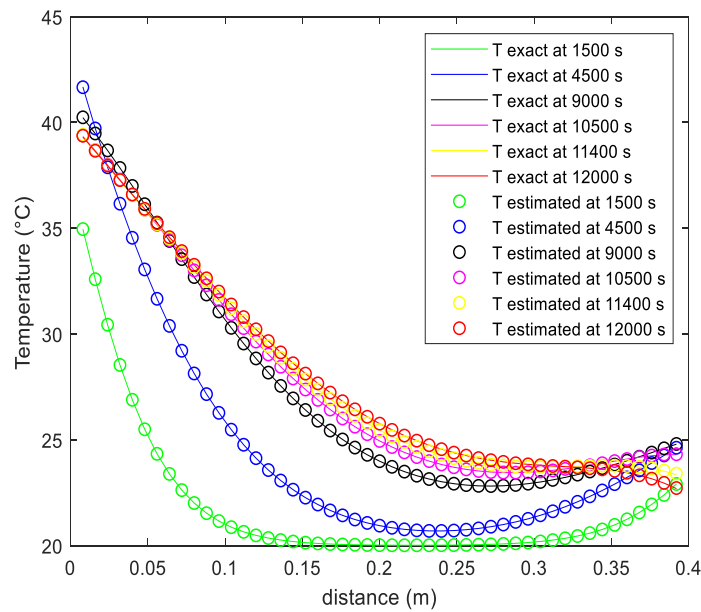

Figure 17. Evolution of temperatures at different time steps by the implicit scheme with variable boundary conditions.
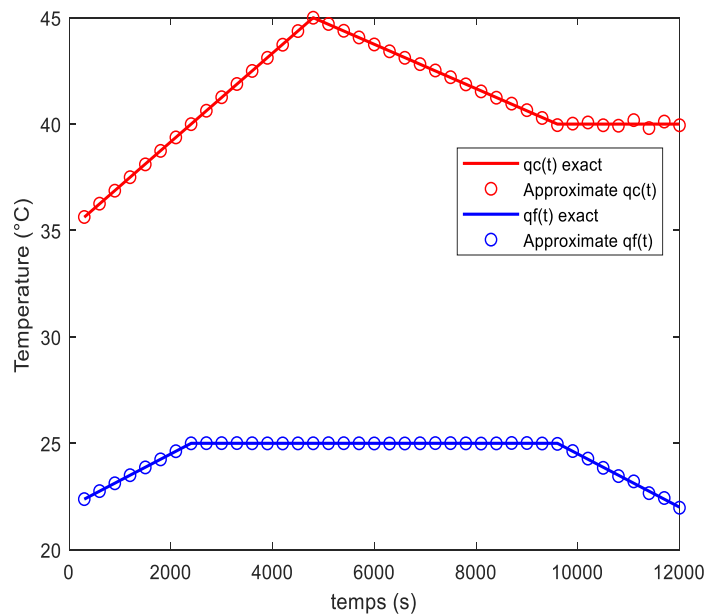

Figure 18. Temperature variations in hot and cold border temperatures.

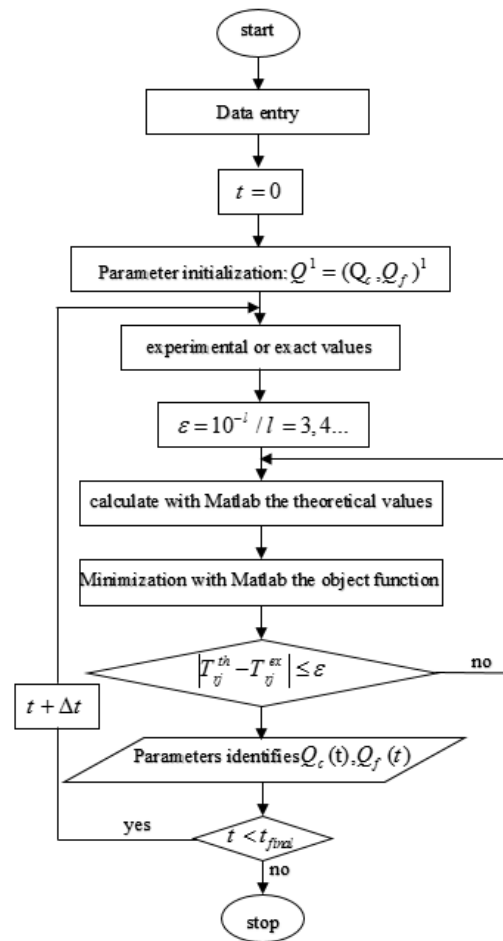The new method is illustrated by the following algorithm, Figure 19:

Figure 19. General simplified algorithm of the main program of the inverse method.

3. Conclusions

The use of the new method (θ-scheme combined with CG method under strong Wolfe line search) in thermal phenomena offers several advantages and a wide scope of applications. It solves many complex problems that cannot be addressed by conventional methods. The method offers extraordinary details (up to 16 digits after the decimal point), and convergence of faster solutions.

In the case of perturbed data, the direct resolution of the θ-scheme will be unstable, therefore this scheme must be regularized.

The conjugate gradient method is a well-known method to alleviate instability by replacing the θ-scheme with an approximate well-posed problem. That is to say, the approximate solution of the θ-scheme is defined as the unique minimizer of the least-squares problem.

The method adopted in this study is therefore a combination of two methods, one for approximation and the other for regularizing the solution.

This procedure can be used to solve direct or inverse problems with total stability of the solutions, especially in the interval $\theta \in]0.5, 1[$. The combination of the scheme and the gradient combined with the strong Wolfe conditions give better solutions within a short time period.

The results of the solution of inverse thermal conduction problems by the scheme technique combined with the conjugate gradient and strong Wolfe conditions compared to the solution of the direct problem of the same stick provide good accuracy and convergence with fast stability and consistent graphics.

The results show that this procedure gives good solutions, namely the constant and/or variable boundary conditions.

The previous results clearly demonstrate the efficacy and reliability of this technique in solving these types of problems. Using this technique, time and space are independent of each other. And above all, this method makes it possible to identify and estimate parameters with high precision in very difficult places, such as the initial properties of materials in the middle of high-temperature ovens or in the middle of freezers. It can also be helpful for surfaces that are difficult to measure, such as in health problems (diseases), free surfaces, parameters in movable surfaces and volumes, and two- and three-phase phenomena (such as smart materials and phase change materials). It also allows for tracking fine trajectories, such as viruses, celestial galaxies, satellite accidents, and climate changes, in addition to predictions and micron distance parameters such as nano, etc.

Author Contributions: Methodology, S.M.E.A.B.; Software, T.B.; Validation, Z.Y.; Data curation, R.D.; Writing—original draft, D.L. All authors have read and agreed to the published version of the manuscript.

Conflicts of Interest: The authors declare no conflict of interest.

Nomenclature

θ:	real number
T:	temperature (°C)
t:	temps (s)
x:	distance (m)
Δt:	time step
Δx:	location step
e or L:	wall thickness (m)
n:	time index
k:	thermal conductivity (w/(m*k))
ρ:	volumic mass (kg/m^3)
Cp:	specific heat (J/(kg*K))
α:	thermal diffusivity (m^2/s)
T_c, q_c:	hot side temperature (°C)
T_f, q_f:	cold side temperature (°C)
CG:	gradient conjugate

References

1. Belgherras, S.; Bekkouche, S.M.A.; Benamrane, N. Prospective analysis of the energy efficiency in a farm studio under Saharan weather conditions. *Energy Build.* **2017**, *145*, 342–353. [CrossRef]
2. Lalmi, D.; Benseddik, A.; Bensaha, H.; Bouzaher, M.T.; Arrif, T.; Guermoui, M.; Rabehi, A. Evaluation and estimation of the inside greenhouse temperature, numerical study with thermal and optical aspect. *Int. J. Ambient. Energy* **2019**, *42*, 1269–1280. [CrossRef]
3. Bekkouche, S.; Benouaz, T.; Hamdani, M.; Cherier, M.; Yaiche, M.; Benamrane, N. Judicious choice of the building compactness to improve thermo-aeraulic comfort in hot climate. *J. Build. Eng.* **2015**, *1*, 42–52. [CrossRef]
4. Bekkouche, S.; Benouaz, T.; Cheknane, A. A modelling approach of thermal insulation applied to a Saharan building. *Therm. Sci.* **2009**, *13*, 233–244. [CrossRef]
5. Carbonari, A.; Naticchia, B.; D'Orazio, M. Innovative Evaporative cooling walls, Eco-Efficient Materials for Mitigating Building Cooling Needs. In *Design, Properties and Applications*; Woodhead: Cambridge, UK, 2015; pp. 215–240. Available online: http://www.sciencedirect.com/science/book/9781782423805 (accessed on 13 December 2022).
6. Stojanovi, B.V.; Janevski, J.N.; Mitkovi, P.B.; Stojanovi, M.B.; Ignjatovi, M.G. Thermally activated building systems in context of increasing building energy efficiency. *Therm. Sci.* **2014**, *18*, 1011–1018. [CrossRef]
7. Mohamed, Z.; Djafer, D.; Chouireb, F. New Approach to Establish a Clear Sky Global Solar Irradiance Model. *Int. J. Renew. Energy Res.* **2017**, *7*, 1454–1462.
8. Rabehi, A.; Guermoui, M.; Lalmi, D. Hybrid models for global solar radiation prediction: A case study. *Int. J. Ambient. Energy* **2018**, *41*, 31–40. [CrossRef]
9. Khelifi, R.; Guermoui, M.; Rabehi, A.; Lalmi, D. Multi-step-ahead forecasting of daily solar radiation components in the Saharan climate. *Int. J. Ambient. Energy* **2018**, *41*, 707–715. [CrossRef]

10. Fang, Z.; Li, N.; Li, B.; Luo, G.; Huang, Y. The effect of building envelope insulation on cooling energy consumption in summer. *Energy Build.* **2014**, *77*, 197–205. [CrossRef]

11. Choi, I.Y.; Cho, S.H.; Kim, J.T. Energy consumption characteristics of high-rise apartment buildings according to building shape and mixed-use development. *Energy Build.* **2012**, *46*, 123–131. [CrossRef]

12. Castellani, B.; Morini, E.; Filipponi, M.; Nicolini, A.; Palombo, M.; Cotana, F.; Rossi, F. Clathrate Hydrates for Thermal Energy Storage in Buildings: Overview of Proper Hydrate-Forming Compounds. *Sustainability* **2014**, *6*, 6815–6829. [CrossRef]

13. Venko, S.; de Ventós, D.V.; Arkar, C.; Medved, S. An experimental study of natural and mixed convection over cooled vertical room wall. *Energy Build.* **2014**, *68*, 387–395. [CrossRef]

14. Tsikaloudaki, K.; Theodosiou, T.; Laskos, K.; Bikas, D. Assessing cooling energy performanceof windows for residential buildings in the Mediterranean zone. *Energy Convers. Manag.* **2012**, *64*, 335–343. [CrossRef]

15. Tsikaloudaki, K.; Laskos, K.; Theodosiou, T.; Bikas, D. The energy performance of windows in Mediterranean regions. *Energy Build.* **2015**, *92*, 180–187. [CrossRef]

16. Guermoui, M.; Abdelaziz, R.; Gairaa, K.; Djemoui, L.; Benkaciali, S. New temperature-based predicting model for global solar radiation using support vector regression. *Int. J. Ambient. Energy* **2019**, *43*, 1397–1407. [CrossRef]

17. Djemoui, L.; Bensaha, H.; Benseddik, A.; Zarrit, R.; Guermoui, M.; Rabehi, A.; Bouzaher, M.T. Comparative study of geometrical configuration at the thermal performances of an agricultural greenhouse. *E3S Web Conf.* **2018**, *61*, 00003. [CrossRef]

18. Tsanasa, A.; Xifarab, A. Accurate quantitative estimation of energy performance of residential buildings using statistical machine learning tools. *Energy Build.* **2012**, *49*, 560–567. [CrossRef]

19. Lalmi, D.; Bezari, S.; Bensaha, H.; Guermouai, M.; Rabehi, A.; Abdelouahab, B.; Hadef, R. Analysis of thermal performance of an agricultural greenhouse heated by a storage system. *Model. Meas. Control B* **2018**, *87*, 15–20. [CrossRef]

20. Lü, X.; Lu, T.; Kibert, C.J. Martti Viljanen a Modeling and forecasting energy consumption for heterogeneous buildings using a physical–statistical approach. *Appl. Energy* **2015**, *144*, 261–275. [CrossRef]

21. Djeffal, R.; Lalmi, D.; Hebbir, N.; Bekkouche, S.M.A.; Younsi, Z. Estimation of Real Seasons in a Semi-Arid Region, Ghardaia, Case Study. *Int. J. Sustain. Dev. Plan.* **2021**, *16*, 1005–1017. [CrossRef]

22. Djeffal, R.; Bekkouche, S.M.A.; Samai, M.; Younsi, Z.; Mihoub, R.; Benkhelifa, A. Effect of Phase Change Material eutectic plates on the electric consumption of a designed refrigeration system. *Instrum. Mes. Métrologie* **2020**, *19*, 1–8. [CrossRef]